Self consistent measurement and removal of the dipolar interaction field in magnetic particle assemblies and the determination of their intrinsic switching field distribution

J. M. Martínez Huerta, J. De La Torre Medina, L. Piraux, and A. Encinas

Citation: Journal of Applied Physics **111**, 083914 (2012);
View online: https://doi.org/10.1063/1.4704397
View Table of Contents: http://aip.scitation.org/toc/jap/111/8
Published by the American Institute of Physics

Self consistent measurement and removal of the dipolar interaction field in magnetic particle assemblies and the determination of their intrinsic switching field distribution

J. M. Martínez Huerta,[1] J. De La Torre Medina,[1,a)] L. Piraux,[2] and A. Encinas[1,3,b)]
[1]*Instituto de Física, Universidad Autónoma de San Luis Potosí, Av. Manuel Nava 6, Zona Universitaria, 78290 San Luis Potosí, SLP, México*
[2]*Institute of Condensed Matter and Nanosciences, Université Catholique de Louvain, Place Croix du Sud 1, B-1348, Louvain-la-Neuve, Belgium*
[3]*División de Materiales Avanzados, Instituto Potosino de Investigación Científica y Tecnológica A. C., Caminio a la Presa 2055, 78216 San Luis Potosí, SLP, México*

(Received 21 November 2011; accepted 15 March 2012; published online 23 April 2012)

Using low density arrays of bistable magnetic nanowires as a model dipolar system, it is shown that the dipolar interaction field coefficient can be measured from the remanence curves as well as from other functions of the isothermal remanent magnetization and the DC demagnetization remanence obtained as an affine transformation of the Wohlfarth relation. Based on mean field arguments, these measurements are used to subtract and remove the contribution of the configuration dependent dipolar interaction field from the major loop and remanence curves. The corrected remanence curves are first used to obtain the intrinsic switching field distribution of the nanowire array and then to validate this approach showing that they yield results consistent with the Wohlfarth relation for an assembly of noninteracting particles, thus providing a self-consistent procedure to verify the measured values of the interaction field and its removal from the measurements. © *2012 American Institute of Physics*. [http://dx.doi.org/10.1063/1.4704397]

I. INTRODUCTION

Dipolar interactions in assemblies of magnetic particles are a central issue in a wide variety of current research topics in magnetism both at the fundamental as well as at the device oriented level. In recent years, very fundamental problems have been at the center of an intense research activity in which an exchange decoupled assembly of nanomagnets is let to interact through the dipolar interaction field. Under different circumstances, this long range and highly anisotropic interaction has revealed a vast set of phenomena and collective effects. For example, artificial magnetic frustration in dipolar nanomagnets, as discussed in Refs. 1 and 2 and references therein. In ultrafine nanoparticle assemblies where depending on the strength of the interaction field, these systems can evolve from weakly coupled superparamagnets where their blocking temperature, coercivity, and remanence show a nontrivial behavior, to strongly coupled assemblies and to show super spin-glass and superferromagnetic ordering, see Refs. 3–5, for excellent reviews on the subject. For highly anisotropic 2D arrays of nanomagnets, the effective field has been shown to depend strongly on the interaction field. For instance it has been shown that in an asymmetrical lattice array dipolar interaction can lead to a magnetostatic anisotropy[6] and that, under adequate conditions, it can even lead to a dipolar induced magnetization reorientation transition as reported for circular dots,[7,8] cylindrical nanowires,[9,10] and planar ellipsoids.[11]

Interacting arrays of single domain nanomagnets are also interesting given the possibility to generate different magnetic states or configurations by selectively switching individual elements, which provides control of the effective field by varying the interaction field that leads to the proposal and realization of configurable/programmable microwave arrays of nanomagnets and magnonic crystals.[12–15]

Individual reversal of dipolar interacting single domain nanomagnets is also the working principle in the development of the quantum magnetic cellular automata and magnetic logic devices.[16–18]

In technological applications of magnetic arrays and assemblies, the dipolar interaction has been suggested as a viable mechanism to enhance the performance of magnetic field magnetoresistance sensors using arrays of coupled parallel rectangular stripes.[19] While for biomedical applications of magnetic nanoparticles, it has been shown that hyperthermia heating efficiency is influenced by the dipolar interaction.[20] In perpendicular magnetic recording, the intrinsic switching field distribution (SFD) is of great importance as it provides a measure of the quality of the recording media.[21–23] In exchange decoupled recording media, the measured SFD differs from the intrinsic one due to a shift of the switching field of individual entities induced by the dipolar interaction, and in recent years a strong effort has been done to find methods that provide a reliable determination of the intrinsic SFD.[23–26]

Determination of the interparticle interaction is a difficult problem both theoretically and experimentally. Experimentally, the most common procedure used to study interaction effects in assemblies of discrete particles rely on plots derived from the Wohlfarth relation,[27] namely, Henkel and ΔM plots.[28,29] Another method often used to study interactions in assemblies

[a)]Current address: Facultad de Ciencias Físico Matemáticas, Universidad Michoacana de San Nicolás de Hidalgo, Avenida Francisco J. Mújica S/N, 58060, Morelia, Michoacán, Mexico.
[b)]Author to whom correspondence should be addressed. Electronic mail: armando.encinas@gmail.com.

of particles is the FORC diagram method.[30] However, although they can provide insight regarding the interaction effects, these methods are qualitative and do not provide the value of the interaction field.

In this sense, only a few methods have been reported that provide a quantitative determination of the interaction field. One of these is the δH plot, also based on the remanence curves.[31,32] More recently two methods have been reported, which provide a direct measure of the interaction field coefficients that are based on the shift of minor loops.[33,34]

In this article, exchange decoupled, low packing arrays of bi-stable NWs are used as a model system to test and validate a method to quantify the dipolar interaction field from their remanence curves. Then based on mean field arguments, the interaction field has been removed from the original hysteresis and remanence curves measurements providing the desheared hysteresis loop and the intrinsic switching field distribution. In order to test the corrected remanence curves, these have been used to construct the m_d vs $1-2m_r$, Henkel and ΔM plots that yield results consistent with assemblies of noninteracting particles. Finally, the dipolar interaction coefficient has been related to the magnetization dependent part of the effective demagnetizing factor for an assembly of particles.

II. EXPERIMENTAL DETAILS

Ni, Co, NiFe, and CoFe nanowires have been grown by electrodeposition into the pores of 21 μm thick lab-made track-etched polycarbonate membranes, in which the pores are parallel to each other but randomly distributed and characterized by their average packing or porosity P.[35] These membranes have improved pore orientation, shape, size distribution, and surface roughness.[36] Full details of the preparation method can be found elsewhere.[37]

For the electrodeposition, a Cr/Au layer is evaporated previously on one side of the membrane to serve as a cathode and deposition is done at a constant potential using a Ag/AgCl reference electrode. For CoFe, a 40 g/l $FeSO_4$ + 80 g/l $CoSO_4$ + 30 g/l H_3BO_3 electrolyte was used with a potential of $V=-0.9$ V, while for NiFe the electrolyte contained 5.56 g/l $FeSO_4$ + 131.42 g/l $NiSO_4$ + 30 g/l H_3BO_3 and deposition is done at $V=-1.1$ V. Cobalt nanowires have been grown at $V=-1$ V using a 238.48 g l^{-1} $CoSO_4$ + 30 g $l^{-1}H_3BO_3$ electrolyte with the pH set to 2.0 by addition of H_2SO_4 to favor a polycrystalline fcc-like Co structure with no magnetocrystalline anisotropy contribution.[38] For all samples, the wire length has been kept between 18 and 20 μm, Table I shows the details of the samples considered.

Magnetometry measurements were performed using an alternating gradient magnetometer, which for the present study included the hysteresis loops along the easy axis as well as DC demagnetization (DCD) and isothermal remanence (IRM) curves, as shown in Figure 1. The IRM curve is measured after the application and removal of an increasingly positive field with the sample initially demagnetized, as indicated by the arrow in Fig. 1. The DCD curve is measured starting from the remanent state obtained after having saturated the sample with a large positive applied field and then by application of increasing negative demagnetizing fields, as shown by the arrow in Fig. 1. All measurements in the present study have been done at room temperature and remanence curves were normalized to the saturation value of the IRM remanence curve.

TABLE I. Wire diameter ϕ and nominal (average) membrane porosity P of the samples used in this study along with the measured values of $H_d^0, H_r^{0.5}$, the interaction field $\alpha = 2(H_r^{0.5} - H_d^0)$ and the rounding ϵ, done on α.

Sample	Material	ϕ (nm)	P (%)	H_d^0(Oe)	$H_r^{0.5}$(Oe)	α(Oe)	ϵ(Oe)
S1	Ni	29	3.6	826	916	180	≤ 1
S2	Ni	30	4.2	760	840	160	1.7
S3	Ni	29	3.5	633	688	110	≤ 1
S4	Co	29	3.7	1400	1500	200	≤ 1
S5	Co	40	0.7	985	1055	140	2.2
S6	Co	39	4.8	1504	1704	400	4
S7	Co	30	3.9	1875	1995	240	3
S8	NiFe	30	3.5	1159	1229	140	≤ 1
S9	NiFe	40	3.4	971	1061	180	≤ 1
S10	CoFe	40	6.4	1711	1911	400	≤ 1
S11	CoFe	29	5.0	1823	2143	640	2.2
S12	CoFe	29	5.0	1333	1593	520	2.5

III. GENERAL CONSIDERATIONS

In this study the system under consideration is a two dimensional assembly of ideally identical particles oriented so that they have their easy axis perpendicular to the layer. The assembly is considered diluted enough to avoid contact between particles so exchange interaction and cooperative processes are neglected. The particles are considered as bistable along the easy axis, so their magnetization can only point in the positive or negative direction along the easy axis and no assumption is made regarding the specific reversal mechanism. Moreover, since all the measurements and the cases of interest consider the applied field to be always directed along the particles easy axis, then the switching field of a given particle approaches the value of its coercive field, so in the following they will be assumed to be equal.[39] Furthermore, all magnetocrystalline anisotropy contributions are neglected, so the system is purely magnetostatic. An assembly of such particles will present dispersion in their specific individual coercive fields that originates in both macro and micro structural inhomogeneities, as discussed in detail in

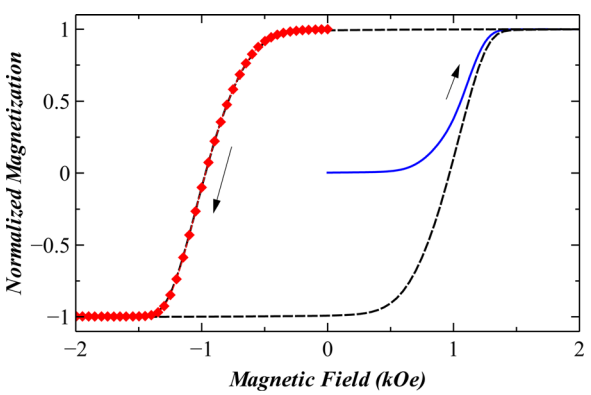

FIG. 1. Major loop, DCD, and IRM remanence curves measured on sample S9 [NiFe].

several references.[21,23,40] This dispersion gives rise to the SFD of the assembly of particles.

In the limit where the assembly is very much diluted and the dipolar interaction field vanishes, the hysteresis loop or any other field induced chance in the magnetic state will take place as the successive reversal of particles according to their intrinsic SFD. Furthermore, for a noninteracting assembly of particles, the normalized DCD (m_d) and IRM (m_r) remanent magnetization curves follow the Wohlfarth relation,[27]

$$m_d = 1 - 2m_r. \tag{1}$$

When the particles are brought closer together the dipolar interaction field between particles is present. In a mean field approach, this field is accounted for by considering that the total field (H_{tot}) acting on a given particle is the sum of the applied field (H_A) and the interaction field taken as the sum of the stray fields produced by all the other particles in the assembly, that is,[21,41,42]

$$H_{tot} = H_A + \alpha m, \tag{2}$$

where $H_{int} = \alpha m$, which is a common expression for the interaction field that has a linear dependence on the magnetic state (m) of the system.[41–46]

This dependence of the total field on the magnetic state introduces a varying term that is zero at coercivity and increases as $|m|$ increases. This additional field will result in a spreading of the measured switching field distribution since every point in the distribution will be shifted in a quantity that is proportional to the value of m. On the other hand, this additional field will also lead to an additional shearing of the hysteresis loop.[21]

To account for the shift of the switching field due to the interaction field, it is necessary to consider that the measured hysteresis loop, as well as any plot of the magnetization, is plotted against the applied field (H_A) and not against the total field H_{tot}. Then, each value of m on the normalized $m - H_A$ plane represents the measured coercive field, H_c, of all the particles having an intrinsic coercive field, $H_{c(i)}$, which is shifted along the field axis by a quantity equal to the dipolar interaction field for that specific value of m. This allows to rewrite Eq. (2) by interpreting the applied field H_A as the measured coercive field H_c and the total field, H_{tot} as the intrinsic coercivity,[47–49]

$$H_{c(i)} = H_c - \alpha m. \tag{3}$$

This expression relates the measured values of the coercive field, H_c, with the intrinsic coercive field denoted as $H_{c(i)}$.

Experimentally, the choice of materials has been based on the following considerations: (1) in order to isolate magnetostatic effects, which in this case includes the shape anisotropy and the dipolar interaction, only arrays of nanowires with negligible magnetocrystalline or magnetoelastic contributions have been considered, (2) small diameter and high aspect ratios ($\geq$ 500, length of 18–20 μm) wires have been used which are expected to be bistable, and (3) low density (low packing) arrays of nanowires have been used to assure a finite interaction field while keeping its value low enough to avoid collective effects such as self-switching, which is reasonably fulfilled with remanences approaching 100%.

IV. RESULTS

A. Measurement of the dipolar interaction field

The Wohlfarth relation, Eq. (1), provides an explicit relation between the IRM and DCD remanence curves that is observed in any assembly of particles when there is no interaction among them and when interactions are present, this relation no longer holds. So the idea is that by determining the difference between the curves measured on the coupled sample and the expected values for the particular case of the noninteracting assembly, one can find the value of the interaction field.

In the mean field approach, every point on the IRM and DCD remanence curves is shifted along the field axis by a quantity that depends on the value of the magnetization, as expressed by Eq.(2), that modifies the curves in a fashion similar to the shearing of the hysteresis loop except for those points where $m = 0$. Indeed, since the interaction field vanishes when $m = 0$, these points in the IRM and DCD curves are the same with or without interaction.

The IRM and DCD curves have a point where $m = 0$. In the IRM remanence curve this point is at the origin, so $m_r = 0, H_a = 0$, and $H_{tot} = 0$. While in the DCD remanence curve, $m_d = 0$ at a field value $H = H_d^0$ (the remanent coercivity), where the curve is not affected, or displaced along the field axis by the interaction field. From Eq. (1) it follows that if there is no interaction, it is required that when the DCD remanence curve passes through $m_d = 0$ at H_d^0, the IRM remanence curve should be at $m_r = 0.5$ at a field value $H = H_r^{0.5}$, so that $H_d^0 = H_r^{0.5}$. If the interaction field is different from zero, then H_d^0 remains unchanged, while the field at which $m_r = 0.5, H_r^{0.5}$ will be shifted with respect to H_d^0 by a quantity equal to $\alpha/2$, so $H_r^{0.5} = H_d^0 + \alpha/2$. That is,

$$H_r^{0.5} - H_d^0 = \Delta H_\alpha = \frac{\alpha}{2}, \tag{4}$$

where it follows that the interaction field coefficient corresponds to

$$\alpha = 2\Delta H_\alpha. \tag{5}$$

This allows to determine the interaction field graphically using directly the IRM and DCD curves to find $H_r^{0.5}$ and H_d^0, as shown in Fig. 2(a) for sample S3. This procedure has been carried out on every sample and the results are given in Table I.

Moreover, ΔH_α can be obtained by plotting as a function of the field any other set of functions of m_d and m_r obtained by performing any affine transformation of the type $ax + b$ on the Wohlfarth relation. For example, plotting together the left (m_d) and right side ($m_r^* = 1 - 2m_r$) of the Wohlfarth relation [Eq. (1)], as a function of the field yields a plot where the interaction effects become evident as both curves are horizontally displaced as shown in Fig. 2(b). Indeed, if there was no interaction, both curves would be identical.

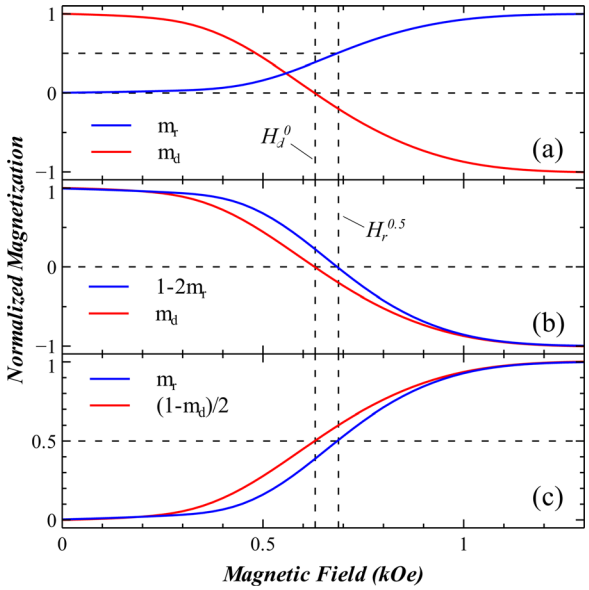

FIG. 2. (a) IRM (m_r) and DCD (m_d) remanence curves measured on Ni sample S3. (b) Modified IRM, $m_r^* = 1 - 2m_r$ and m_d remanence curves as a function of the field and (c) modified DCD, $m_d^* = (1 - m_d)/2$ and m_r remanence curves as a function of the field.

Another example, shown in Fig. 2(c), would be to solve Eq. (1) for m_r and to plot m_r along with the modified DCD, $m_d^* = (1 - m_d)/2$, that leads to plots that allow to observe the presence of the interaction field. As seen from Figs. 2(b) and 2(c), ΔH_α can be graphically determined once the corresponding field values for $m_d = 0$ and $m_r = 1/2$ are found, as shown by the vertical dashed lines. Another example of these types of plots are those reported by Harrell *et al.*[32] that, in terms of the variables used here, plots $-m_d$ and $-m_r^*$.

In the following, $m_r^* = 1 - 2m_r$ will be referred to as the modified IRM and the plot shown in Fig. 2(b) will be referred to as the m_r^*/m_d plot.

B. Deshearing of the hysteresis loop and intrinsic switching field distribution

The dipolar interaction in assemblies of particles plays an important role in two basic and well known measured characteristics which are always present in magnetization measurements, the shearing of the hysteresis loop and the broadening of the switching field distribution.

It is well known that any finite object when subject to an applied magnetic field, it will also experience the field produced by its magnetic poles, which calls for the use of the self-demagnetizing factor to take this contribution into account, and is responsible for the shearing of the hysteresis loop. However, when considering an assembly of particles, each particle is subjected to its own demagnetizing field and also to the stray field produced by all the other particles in the assembly. This additional field corresponds to the dipolar interaction field, which opposes the magnetization of a given particle, and thus results in an additional shearing of the hysteresis loop. The standard mean field approach to account for these contributions is to introduce an effective demagnetizing factor N_{eff}, which includes both demagnetizing effects, the self-demagnetizing field of the particle and the dipolar interaction field experienced by the particle. The complications in determining N_{eff} in a real assembly of particles follow from the fact that the value of the interaction field is unknown, so it's not possible to find how much shearing is due to this field. While, on the other hand, there is a finite shearing of the hysteresis loop due to the statistical dispersion of the self demagnetizing field of the particles, or, equivalently, due to the intrinsic SFD. Then the problem is to determine one quantity, N_{eff}, that depends on these two unknown variables.

However, knowledge of the interaction field simplifies the problem, since one can expect that this contribution can be subtracted or removed from the measured hysteresis loop, leading to the intrinsic loop of the assembly. Regarding the M(H) loop as a plot of the magnetization changes resulting from a total field that includes the applied as well as the interaction field, plotted against the applied field, then the corrected hysteresis loop follows from plotting the magnetization as a function of the field once the dipolar interaction is subtracted, according to Eq. (3). Figure 3 shows the results of these corrections on the major loop, in each case the as-measured loop (dashed line) is compared with the corrected, or desheared, loop (continuous line), for samples (a) S3, (b) S5, (c) S9, and (d) S11. In all cases, the value of the interaction field has been measured using the method presented in Sec. IV A, and corresponds to those indicated in Table I for each sample. The correction is performed by recalculating the field for each point in the plot using Eq. (3) and plotting the as-measured magnetization against this field. As can be seen from the results, in all cases the correction performed leads to more square loops and no over deshearing is observed. Furthermore, as expected, the coercive field remains unchanged upon performing the correction, in agreement with Eq. (3) in which the interaction field vanishes at the coercive field. These corrected hysteresis loops correspond to the intrinsic loops of the assembly once the effects

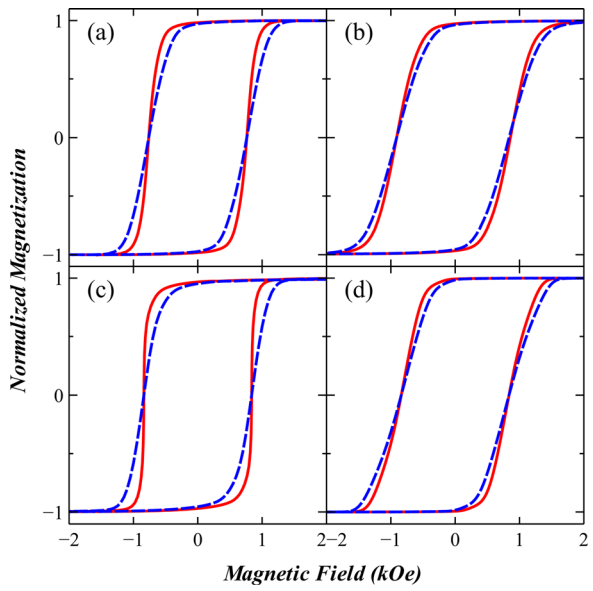

FIG. 3. Hysteresis deshearing of 4 different nanowires samples: (a) S3 [Ni], (b) S5 [Co], (c) S9 [NiFe], and (d) S11 [CoFe], the measured and corrected cycles are shown with dashed and continuous lines, respectively.

of the dipolar interaction have been removed. The extent to which this corrected M(H) loops are correct, is considered in the following sections.

Due to its technological relevance, there is great interest in finding methods to determine the intrinsic switching field distribution in assemblies of particles as well as in patterned media. The problem regarding its determination is the same as the one described above for the effective demagnetizing factor, this is, the intrinsic properties of the assembly are measured superposed with the interaction field contributions. However, if the dipolar field interaction is removed from the as measured switching field distribution, the result would yield the intrinsic SFD.

For perpendicular media, the SFD is obtained as the differentiated DCD curve,[24,25] and only when the DCD curve and the major loop coincide can the SFD be considered as the differentiated major loop.[50]

To obtain the intrinsic switching field distribution, Eq. (3) has been used to calculate the corrected DCD ($m_{d'}$) curve using the values of the interaction field given in Table I. The intrinsic SFD follows from direct derivation of $m_{d'}$ with respect to the applied field. Figure 4 shows the comparison between the normalized as-measured SFD and the intrinsic SFD obtained for samples S3, S6, S8, and, S10.

From these comparisons, the intrinsic SFD shows a clear difference with respect to the as-measured SFD. In particular, the width of the distribution is clearly reduced in all cases. An interesting feature of these results is that, as seen from Figs. 4(b) and 4(c), the particular features of the as-measured SFD are preserved in the intrinsic SFD. For these cases, the as-measured SFD clearly shows two shoulders indicative of complex switching mechanisms that can originate from several features such as an structural inhomogeneity, for example mixtures of crystalline phases; or variations of the wire density which result in a variation of the interaction field. An important feature is that since the intrinsic SFD is obtained by a direct transformation of the as-measured SFD, no fitting procedures are required and there is no need to assume any particular functional form for the intrinsic SFD which could lead to neglecting specific features of the distribution.

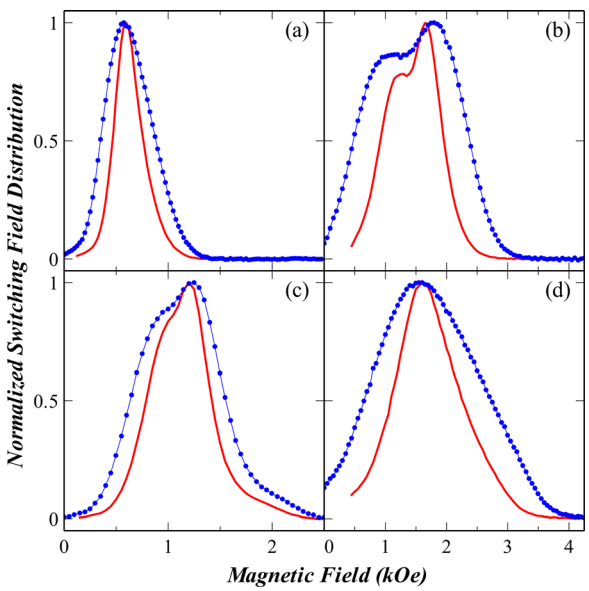

FIG. 4. As-measured SFD (filled circles with line) compared with the intrinsic SFD (continuous line) obtained for samples (a) S3 [Ni], (b) S6 [Co], (c) S8 [NiFe], and (d) S10 [CoFe].

C. Approximation validity

As shown in Sec. IV B, the use of Eq. (5) to measure the interaction field and Eq. (3) to remove it from the measurements provides reasonable results since no over-deshearing has been obtained and the intrinsic SFD is narrower than the as-measured SFD. However, it is natural to ask about the correctness and the validity of these assumptions since the method does not provide a proof that the resulting desheared hysteresis loop or the intrinsic SFD are in fact correct.

In order to test and validate if the dipolar interaction field is effectively and accurately removed from the measurements, a comparison between the as measured data and those obtained after removal of the dipolar interaction field is made. The aim is to use the m_r^*/m_d, Henkel and ΔM plots to verify if the corrected DCD and IRM remanence curves lead to the well known limit of an assembly of non interacting particles that follow the Wohlfarth relation.

To construct these plots, it was necessary to use a numerical interpolation procedure in the as-measured data sets in order to have exactly the same field values for every point in $m_d(H)$ and $m_r(H)$. This procedure was done in all the measurements, and in all cases the original and interpolated data sets were compared to verify that they provided identical remanence curves. Then the corrected $m_{d'}$ and $m_{r'}$ were calculated using Eq. (3) using the values for the interaction field given in Table I.

1. m_r^*/m_d plots

As a first method used to test the accurate removal of the interaction field based on Eq. (3), the remanence curves are tested with the m_r^*/m_d plot. As mentioned before, m_d and the modified IRM taken as $m_r^* = 1 - 2m_r$ are plotted as a function of the field. In this case, if there is no interaction both plots are identical; on the contrary, when there is an interaction between particles, the plots are horizontally displaced as a result of this interaction field.

Figure 5 shows the m_r^*/m_d plots for three different arrays of NWs, S3, S5, and S9, on the left side the as-measured plots, and on the right side the plots obtained once the dipolar interaction field is removed. As expected, the results shown in Figs. 5(a) S3, 5(c) S5, and 5(e) S9, the as measured m_d and $m_r^* = 1 - 2m_r$ plots can be clearly distinguished due to the presence of a dipolar interaction field.

By removing the interaction field from the as measured IRM and DCD remanence curves using Eq. (3), and the interpolation procedure described above for plotting corrected $m_{d'}$ and $m_{r'}^* = 1 - 2m_{r'}$ remanence curves, it can be seen from Figs. 5(b), 5(d), and 5(f), for samples S3, S5, and S9, respectively; that both $m_{d'}$ and $1 - 2m_{r'}$ are practically identical over the entire field range, consistent with the limit of the noninteracting assembly of particles, providing a positive confirmation of both, the measurement of the interaction field and the mean field approach expressed by Eq. (3).

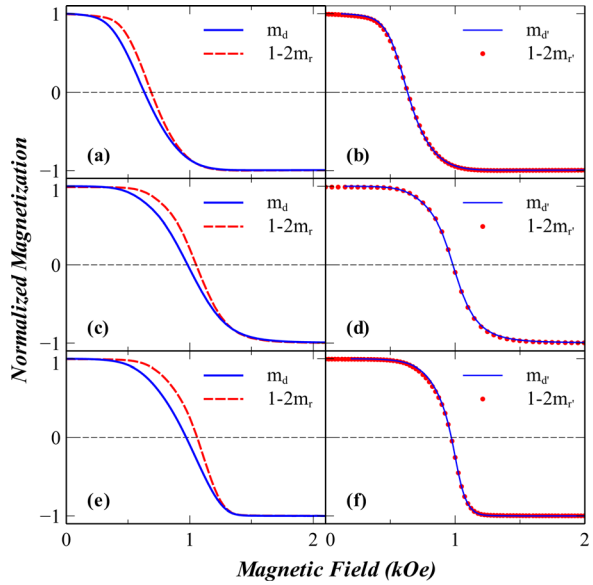

FIG. 5. m_r^*/m_d plots obtained from the as-measured and corrected DCD and IRM remanence curves for samples S3-Ni [(a) and (b)], S5-Co [(c) and (d)], and S9-NiFe [(e) and (f)].

2. Henkel plots

In the Henkel plots m_d is plotted as a function of m_r, for a noninteracting assembly of particles, this corresponds to a straight line given by Eq. (1).[28] Interactions among particles can be identified when the measured Henkel plot shows deviations from the ideal Henkel line. When the deviations lie below this line, it corresponds to an antiferromagnetic type interaction. On the contrary, deviations above this line correspond to a ferromagnetic type interaction.

Figure 6 shows the Henkel plots, from the as-measured data compared to those corrected after subtraction of the configuration dependent dipolar interaction field for samples (a) S4, (b) S8, and (c) S12, as a reference the Henkel plot for the non-interacting assembly is shown as a dashed line.

As expected, the as-measured Henkel plots show a clear deviation with the non-interacting Henkel plot (dashed line), consistent with a dipolar interaction field. Comparing now the Henkel plots obtained using the corrected IRM and DCD, it is clear that the deviation is removed leading to a result consistent with an array of noninteracting particles as was expected.

3. ΔM plots

The ΔM plots are another analysis method based on the Wohlfarth relation that provides information about the interactions in an assembly of particles.[29] In particular, rewriting the Wohlfarth relation, Eq. (1), ΔM is defined as

$$\Delta M = 2m_r - m_d - 1. \tag{6}$$

Where it follows that for the assembly of non-interacting particles $\Delta M = 0$ for all field values, and the deviations from zero show the presence of an interaction which can be antiferromagnetic type (negative deviation) or ferromagnetic type (positive deviation).

Figure 7 compares the as-measured (continuous line) and the corrected (dashed line) ΔM plots for samples (a) S1, (b) S5, and (c) S9. As seen from these results, the as-measured plots are consistent with a dipolar interaction field as the ΔM deviations are always negative. On the other hand, it can also be observed that the corrected plots are, to a very good degree, consistent with the limit of the noninteracting assembly of magnetic particles. Indeed, in all the cases shown in Fig. 7, the corrected ΔM plots are very close to zero for all field values, proving that the removal of the dipolar interaction field is done correctly. However, from these results it can be noticed that the corrected plots are not strictly equal to zero, and small deviations are present.

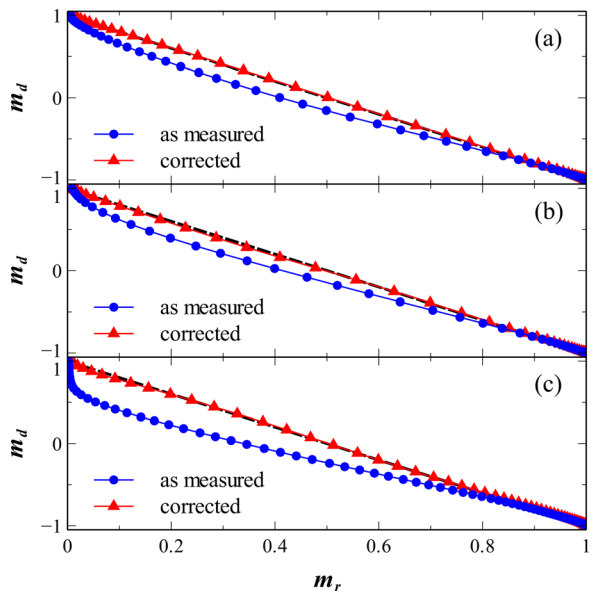

FIG. 6. Comparison of the as measured and the corrected Henkel plots for samples (a) S4 [Co], (b) S8 [NiFe], and (c) S12 [CoFe], as a reference the Henkel plot of the non-interacting assembly is shown as a dashed line.

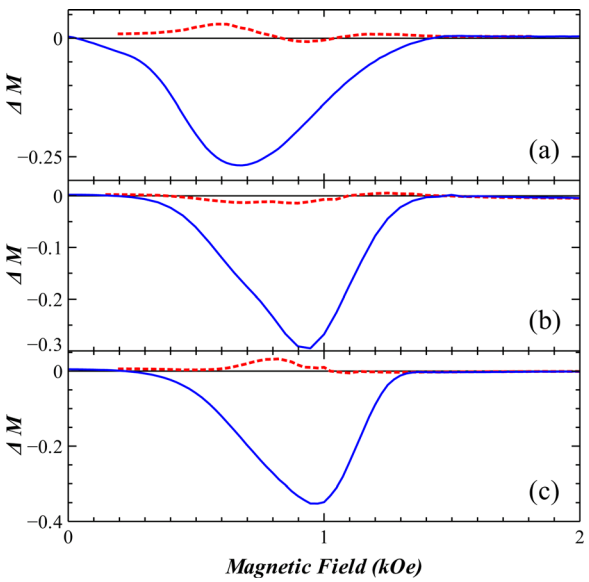

FIG. 7. ΔM plots obtained from the as-measured (continuous line) and corrected (dashed line) IRM and DCD remanence curves, for samples (a) S1 [Ni], (b) S5 [Co], and (c) S9 [NiFe].

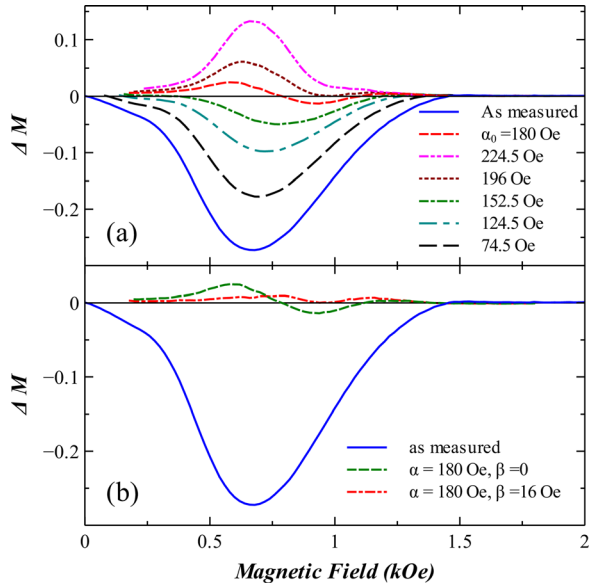

FIG. 8. (a) ΔM plots obtained from the as-measured and corrected (for different values of H_{int}) IRM and DCD remanence curves, and (b) ΔM plots obtained using the second order mean field term [Eq. (7)] for sample S1 [Ni].

In order to have more insight into this feature, the ΔM plots have also been determined by varying numerically the values for the dipolar interaction field with respect to the one determined experimentally (α_0). Figure 8(a) shows the results obtained for sample S1.

As seen from this figure, the corrected ΔM plots show clear changes as a function of the value of the interaction field. Firstly, the corrected plot obtained using the measured value of the interaction field, α_0, shows a clear deviation from zero, taking both positive and negative values. This would suggest that even for small errors in the value of the interaction field, the ΔM plot show deviations from zero.

If the value of the interaction field is varied then the corresponding plots change sensibly, even for relatively small reductions of the interaction field the changes in the deviations are significant. For example, using a change as small as 27.5 Oe, we notice that the ΔM plot for $\alpha = 152.5$ Oe shows a large deviation from the one corresponding to $\alpha_0 = 180$ Oe.

If the value of the interaction field is increased, the changes in the ΔM plots take place in the opposite sense. This is, if the interaction field becomes too large, then ΔM becomes positive, as seen in the figure, where even a small increase of $\approx$16 Oe from $\alpha_0 =$180 Oe to $\alpha =$196 Oe, results in significant positive deviations from zero.

These results show that the ΔM plots are very sensitive to the values used for the interaction field. Moreover, it would seem that even for correct values of the interaction field, small deviations and crossover behaviors around the values for the ideal non-interacting assembly are to be expected.[46] To gain more insight to the presence of these deviations an expression with a higher order term for the mean field dipolar interaction field has been considered. Namely, the expression used by Che and Bertram has been used, that is,[45]

$$H_{int} = \alpha m + \beta(1 - m^2), \tag{7}$$

where the first term corresponds to the first order mean field approximation used so far, while the second order term accounts for the fluctuations of the interaction field.[45] The procedure used, began with using the measured value for the first order term, and keeping this value constant, the IRM and DCD remanence curves were recalculated for different values of β starting at zero and increasing at steps of 2 Oe. Figure 8(b) shows the ΔM plots calculated with the as-measured remanence curves, and those giving the best results using only the linear term ($\alpha = 180$ Oe and $\beta = 0$) and that with the second order term ($\alpha =$ 180 Oe and $\beta = 16$ Oe), for sample S1.

The results show that by introducing the second order term the corrected ΔM plot approaches significantly to zero. However, one can observe the persistence of small deviations from zero, so with this simple model, Eq. (7), some improvement is obtained but deviations from zero persist. This suggest that the first linear term is not necessarily enough to completely remove the effects of the interaction, and that the fluctuations of the dipolar field might be of some relevance even for diluted systems as the ones considered here. From the results of various calculations, the values of the coefficient β of the second order term are systematically an order of magnitude smaller than the coefficient α of the first order term, which seems reasonable since fluctuations of the dipolar interaction field are expected to rise due to dispersion in wire length and on their exact positions.

V. DISCUSSION

From the previous sections, the results obtained with the m_r^*/m_d, Henkel and ΔM plots, provide a self-consistent method to verify that the measured values of the interaction field as well as the mean field approach expressed by Eq. (3) is correct. In all cases, the results show a very good agreement with those expected for an assembly of non-interacting particles, and small improvements can further be attained by using a second order expression for the interaction field. In comparison with other methods recently proposed to measure the interaction field,[33,34] the method presented here has the natural advantage that it relies on the DCD and IRM remanence curves, and not on recoil loop measurements, so it inherently eliminates the effects or contributions coming from reversible processes present in the measurements.

In this sense it is interesting to note that $\alpha = 2\Delta H_\alpha$ is closely related to the interaction field factor (IFF) introduced by Corradi and Wohlfarth,[51] considered as a measure of the interactions in an assembly of particles. This unit-less quantity is defined as $H_r^{0.5} - H_d^0$ [Eq. (4)] normalized by the coercive field of the sample,[45,52] and only provides qualitative information on the type of interaction present. Similar to the Henkel and ΔM plots, the type of interaction is deduced from its sign and IFF = 0 for the non-interacting case. The main difference between the IFF and the value of the interaction field coefficient, Eq. (5), is the factor 2 preceding ΔH_α that follows from the mean field considerations and the expression for the total field [Eq. (2)].

The results presented also provide verification that the determined intrinsic switching field distribution is correct. Regarding the determination of the intrinsic SFD, an important

characteristic of the present results, contrary to other methods,[25,26] is that no assumption is required on the functional form of the intrinsic SFD, and no numerical procedures are required.[53] This is a key feature, since it naturally provides detailed information of the intrinsic SFD such as the presence of more than one peak in the distribution.

For the applicability of the method used for the measurement of the interaction field, the only assumptions made is that no collective effects take place and that the interaction field varies linearly with the total magnetization of the assembly, which implicitly considers that the interaction field coefficient, α, is constant, consistent for an assembly of non-touching (exchange decoupled) particles having only dipolar interaction.[54] Furthermore, in the mean field approach, the interaction field coefficient can include both dipolar and exchange interactions. However the use of this approximation is limited to low and moderate values of α, since for large values the mean field model yields unphysical results such as overskewing and unreasonably large coercivities.[55] Where the limiting value of α is determined by the onset of collective effects, which will depend on the value of the effective uniaxial anisotropy of the particles in the assembly, that determines the extent to which the particles (or grains) can be considered as independent.

Experimentally, there are also restrictions on the use of the IRM and DCD remanence curves as discussed in Refs. 56 and 57, which show that the accuracy of the results obtained from the standard IRM and DCD remanence curves is limited to those cases in which the material remanence is high. This restricts the use of the remanence curves in materials with low or negligible magnetocrystalline anisotropy to those cases where the interaction field remains low. However, in magnetic materials used for perpendicular magnetic recording, a strong uniaxial magnetocrystalline anisotropy is usually present, which will further contribute to ensure a high remanence while minimizing the effect of the dipolar interaction field.[40,58]

As mentioned in the previous sections, under mean field considerations; in an assembly of particles the effective demagnetizing field, $\vec{H}^D_{eff} = N_{eff} \cdot \vec{M}$, contains two contributions, one associated with the self demagnetizing factor of the particles, $\vec{H}^D_{self}$ and the other due to the stray field of the other particles in the assembly, namely, $\vec{H}^D_{int}$. So that $\vec{H}^D_{eff} = \vec{H}^D_{self} + \vec{H}^D_{int}$.

In the limit of very low density, the interaction field vanishes, and the effective demagnetizing field reduces to that of the single isolated particle, $\vec{H}^D_{eff} = \vec{H}^D_{self}$. While the measured dipolar interaction field coefficient, α, is related to $\vec{H}^D_{int}$. Specifically, since α has been measured with the field applied parallel to the wires, the z-axis, then, along this component $\alpha = H^D_{int}$. When the system is saturated along the z-axis $H^D_{int} = M_s N^D_{int}$, where it follows that the interaction demagnetizing factor is

$$N^D_{int} = \frac{\alpha}{M_s}. \tag{8}$$

This expression relates the measured interaction field coefficient with the magnetization dependent part of the effective demagnetizing factor that results from the dipolar interaction among the particles that make up the assembly.

VI. CONCLUSIONS

In conclusion, based on high remanence arrays of bistable magnetic nanowires a method to measure the dipolar interaction field based on remanence curve measurements has been proposed and validated. While using mean field arguments this interaction has been removed from the as measured hysteresis loops and remanence curves, leading to the deshearing of the hysteresis loop and the determination of the intrinsic switching field distribution. The measurement of the interaction field as well as its correct removal from the as measured data has been verified by checking that the corrected data follow the Wohlfarth relation for an assembly of noninteracting particles. Finally, the interaction field coefficient has been related to the magnetization dependent part of the effective demagnetizing factor for an assembly of particles. This methodology provides a simple approach to determine both the value of the interaction field and the intrinsic switching field distribution without the need of guessing the functional form of the distribution and with a self consistent check of the results that can be of interest for the characterization of exchange decoupled assemblies of nanomagnets.

ACKNOWLEDGMENTS

The authors thank R. Legras and E. Ferain for providing the PC membranes. This work was partly supported by the Interuniversity Attraction Poles Program (P6/42)—Belgian State—Belgian Science Policy and CONACYT México project CB 105568. J. M. Martínez Huerta thanks CONACYT for scholarship 201754 and J. De La Torre thanks PROMEP and CONACYT for financial support through grants No. PROMEP/103.5/11/2159 and No. 166089, respectively.

[1]N. Rougemaille *et al*., Phys. Rev. Lett. **106**, 057209 (2011).
[2]S. Zhang *et al*. Phys. Rev. Lett. **107**, 237202 (2011).
[3]S. A. Mejetich and M. Sachan, J. Phys. D: Appl. Phys. **39**, R407 (2006).
[4]M. Knobel, W. C. Nunes, L. M. Socolovsky, E. De Biasi, J. M. Vargas, and J. C. Denardin, J. Nanosci. Nanotechnol. **8**, 2836 (2008).
[5]S. Bedanta and W. Kleemann, J. Phys. D: Appl. Phys. **42**, 013001 (2009).
[6]R. P. Cowburn, A. O. Adeyeye, and M. E. Welland, New J. Phys. **1**, 161 (1999).
[7]K. Yu Guslienko, Appl. Phys. Lett. **75**, 394 (1999).
[8]K. Yu Guslienko, S.-B. Choe, and S.-C. Shin, Appl. Phys. Lett. **76**, 3609 (2000).
[9]M. Lederman, R. O'Barr, and S. Scultz, IEEE Trans. Magn. **31**, 3793 (1995).
[10]A. Encinas-Oropesa, M. Demand, L. Piraux, I. Huynen, and U. Ebels, Phys. Rev. B **63**, 104415 (2001).
[11]S. Jain, A. O. Adeyeye, and N. Singh, Nanotechnology **21**, 285702 (2010).
[12]A. Encinas, L. Vila, M. Darques, J.-M. George, and L. Piraux, Nanotecnology **18**, 065705 (2007).
[13]L. P. Carignan, A. Yelon, D. Menard, and C. Caloz, IEEE Trans. Microwave Theory Tech. **59**, 2568 (2011).
[14]J. Topp, D. Heitmann, M. P. Kostylev, and D. Grundler, Phys. Rev. Lett. **104**, 207205 (2010).
[15]J. Ding, M. Kostylev, and A. O. Adeyeye, Phys. Rev. Lett. **107**, 047205 (2011).
[16]R. P. Cowburn and M. E. Welland, Science **287**, 1466 (2000).
[17]D. A. Allwood, Gang Xiong, M. D. Cooke, C. C. Faulkner, D. Atkinson, N. Vernier, and R. P. Cowburn, Science **296**, 2003 (2002).

[18]A. Imre, G. Csaba, L. Ji, A. Orlov, G. H. Bernstein, and W. Porod, Science **311**, 205 (2006).
[19]B. B. Pant, J. Appl. Phys. **79**, 6123 (1996).
[20]D. Serantes *et al*., J. Appl. Phys. **108**, 073918 (2010).
[21]H. J. Richter, J. Phys. D: Appl. Phys. **40**, R149 (2007).
[22]B. D. Terris, J. Magn. Magn. Mater. **321**, 512 (2009).
[23]J. W. Lau and J. Shaw, J. Phys. D: Appl. Phys. **44**, 303001 (2011).
[24]R. J. M. van de Veerdonk, X. Wu, and D. Weller, IEEE Trans. Magn. **38**, 2450 (2002).
[25]R. J. M. van de Veerdonk, X. Wu, and D. Weller, IEEE Trans. Magn. **39**, 590 (2003).
[26]A. Berger, B. Lengsfield, and Y. Ikeda, J. Appl. Phys. **99**, 08E705 (2006).
[27]E. P. Wohlfarth, J. Appl. Phys. **29**, 595 (1958).
[28]O. Henkel, Phys. Status Solidi **7**, 919 (1964).
[29]P. E. Kelly, K. O'Grady, P. I. Mayo, and R. W. Chantrell, IEEE Trans. Magn. **25**, 3881 (1989).
[30]R. Pike, A. P. Roberts, and K. L. Verosub, J. Appl. Phys. **85**, 6660 (1999).
[31]R. J. Veitch, IEEE Trans. Magn. **26**, 1876 (1990).
[32]J. W. Harrell, D. Richards, and M. R. Parker, J. Appl. Phys. **73**, 6722 (1993).
[33]T. Wang, Y. Wang, Y. Fu, T. Hasegawa, H. Oshima, K. Itoh, K. Nishio, H. Masuda, F. S. Li, H. Saito, and S. Ishio, Nanotechnology **19**, 455703 (2008).
[34]A. N. Dobrynin, T. R. Gao, N. M. Dempsey, and D. Givord, Appl. Phys. Lett. **97**, 192506 (2010).
[35]The porosity P is defined as the surface filling fraction and is obtained as the product of the density of pores and the pore area.
[36]E. Ferain, and R. Legras, Nucl. Instrum. Methods Phys. Res. B **131**, 97 (1997).
[37]L. Piraux, A. Encinas, L. Vila, S. Mátéfi-Tempfli, M. Mátéfi-Tempfli, M. Darques, F. Elhoussine, and S. Michotte, J. Nanosci. Nanotechnol. **5**, 376 (2005).
[38]M. Darques, A. Encinas, L. Vila, and L. Piraux, J. Phys. D: Appl. Phys. **37**, 1411 (2004).
[39]A. Ghaddar, F. Gloaguen, J. Gieraltowski, and C. Tannous, Physica B **406**, 2046 (2011).
[40]J. W. Lau, R. McMichael, S. H. Chung, J. O. Rantschler, V. Parekh, and D. Litvinov, Appl. Phys. Lett. **92**, 012506 (2008).
[41]G. Bertotti, *Hysteresis in Magnetism* (Academic Press, London, 1998), pp.134–135.
[42]J. Geshev and J. E. Schmidt, IEEE Trans. Magn. **33**, 2504 (1997).
[43]D. C. Jiles and D. L. Atherton, J. Magn. Magn. Mater. **61**, 48 (1986).
[44]D. L. Atherton and J. R. Beattie, IEEE Trans. Magn. **26**, 3059 (1990).
[45]X.-D. Che and N. Bertram, J. Magn. Magn. Mater. **116**, 121 (1992).
[46]E. Della Torre, *Magnetic Hysteresis* (IEEE Press, New York, 1999), p. 77
[47]Y. D. Yan and E. Della Torre, J. Appl. Phys. **67**, 5370 (1990).
[48]M. Pardavi-Horvath, Guobao Zheng, G. Vertesy, and A. Magni, IEEE Trans. Magn. **32**, 4469 (1996).
[49]M. Parvadi-Horvat, Mater. Res. Soc. Symp. Proc. **674**, U4.6 (2001).
[50]D. Litvinov, V. Parekh, E. Chunsheng, D. Smith, J. O. Rantschler, P. Ruchhoeft. D. Weller, and S. Khizroev, IEEE Trans. Nanotechnol. **7**, 463 (2008).
[51]A. R. Corradi and E. P. Wohlfarth, IEEE Trans. Magn. **14**, 861 (1978).
[52]R. W. Chantrell, K. O'Grady, J. Phys. D: Appl. Phys. **25**, 1 (1992).
[53]M. Winklhofer and G. T. Zimanyi, J. Appl. Phys. **99**, 08E710 (2006).
[54]X. Wu, and R. J. M. van de Veerdonk, IEEE Trans. Magn. **44**, 336 (2008).
[55]R. Skomski, J. Phys.:Condens. Matter **15**, R841 (2003).
[56]E. O. Samwel, P. R. Bissell, and J. C. Lodder, J. Appl. Phys. **73**, 1353 (1993).
[57]J. G. Th. te Lintelo and J. C. Lodder, J. Appl. Phys. **77**, 6416 (1995).
[58]W. F. Brown, Jr., *Magnetostatic Principles in Ferromagnetism* (North-Holland, Amsterdam, 1962), p. 112.